

The Austenitic Start and Finish Temperature
of a
 $\text{Ni}_{55}\text{Ti}_{45}$ Compression Spring

Derek Dunlap
Haiyong Li

December 14, 2002

Submitted in Partial Fulfillment of course requirements for
MatE 210 – Fall 2002 Instructor Professor Guna Selvaduray

TABLE OF CONTENTS

LIST OF FIGURES.....	iii
LIST OF TABLES.....	iii
ABSTRACT.....	iv
1.1 INTRODUCTION.....	1
1.1.1 THEORY.....	1
1.1.2 CRITICAL REVIEW OF PREVIOUS WORK.....	2
1.2 EXPERIMENTAL.....	6
1.2.1 Experimental Setup.....	6
1.2.2 Experimental Procedure.....	8
1.3 RESULTS.....	9
1.4 DISCUSSION.....	11
1.4.1 STATISTICAL ANALYSIS.....	11
1.4.2 SOURCE OF ERRORS.....	12
1.5 CONCLUSION.....	13
1.6 ACKNOWLEDGEMENTS.....	14
1.7 REFERENCES.....	14
APPENDIX.....	17

LIST OF FIGURES

Figure 1. Crystal form change that leads to shape memory effect	1
Figure 2. A typical DSC curve for NiTi Shape Memory Alloy.....	3
Figure 3. A typical active A_f test curve	5
Figure 4. A typical strain recovery test curve	6
Figure 5. Schema for the experiment setup	7
Figure 6. Actual experiment setup.....	7
Figure 7. Transformation curve for $Ni_{55}Ti_{45}$ compression after 10.1 cm elongation	9
Figure 8. Graphic method used to determine A_s and A_f	10
Figure 9. Transformation curve for $Ni_{55}Ti_{45}$ compression after 10.1 cm elongation	11

LIST OF TABLES

Table 1. Calculation results for A_s and A_f	11
---	----

ABSTRACT

The austenitic start and finish temperature was determined for a Ni₅₅Ti₄₅ compression spring. The spring was elongated at two different lengths then various currents were applied to the spring with a DC power supply. A thermocouple was used to measure the temperature at specific current intervals. When a change in shape and a steady state of temperature was observed the temperature was recorded. A plot was then created to determine the austenitic start and finish temperature.

1.1 Introduction

1.1.1 Theory

The shape memory effect (SME) appears in some special alloys that show crystallographically reversible martensitic transformations. When mechanical load is applied to the material in the state of twinned martensite, it is possible to detwin the martensite. Upon releasing of the load, the material remains deformed. A subsequent heating of the material to a temperature above the reverse-transformation finish temperature (A_f) will lead to complete shape recovery, as shown in Figure 1. The above described process results in manifestation of the shape memory effect.

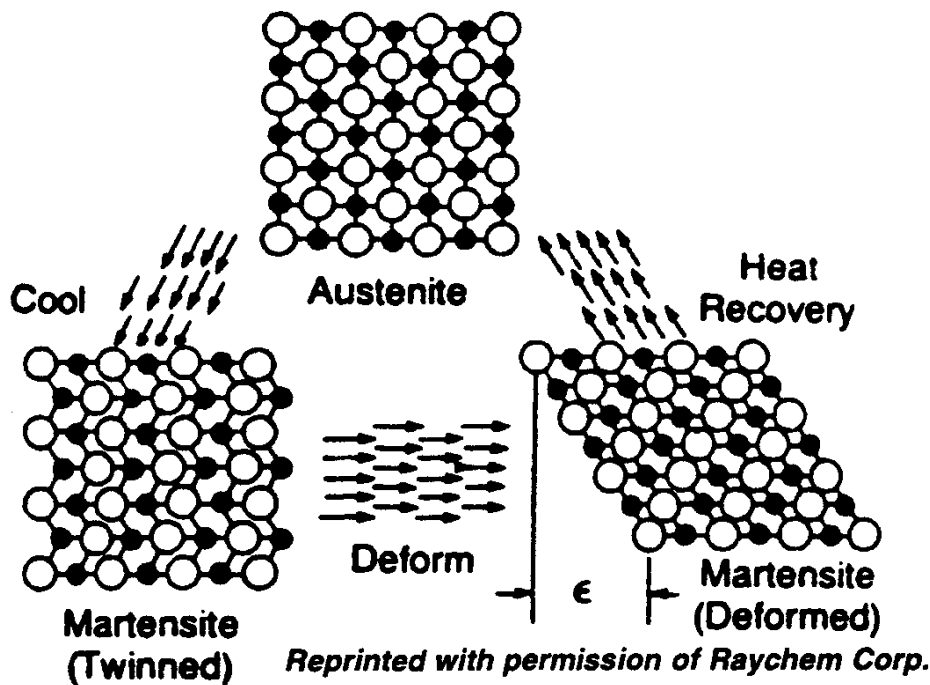


Figure 1: Representation of the changes in the crystal form of shape memory alloys that leads to the shape memory effect [1]

Shape memory effect was first discovered in AuCd alloy in 1932 [2]. However, the research in this field did not really become extensive until similar behavior was found in a less exotic NiTi alloy (Nitinol) in 1963. Many kinds of shape memory alloys have subsequently been developed, but only NiTi alloys, copper-base alloys, and Shape Memory Stainless Steel (SMSS) have been commercially exploited [3]. Among these three groups, NiTi alloy has been the most important material for applications, because the Cu-based alloys are brittle in a polycrystalline state [4], and the fully reversible strain of the SMSS is comparatively small [5]. Today, applications utilizing the shape memory effect in NiTi alloys have penetrated various market sectors such as the connector, household appliance, and biomedical fields [6].

Successful development of any applications involving shape memory effect requires a clear understanding of the transformation temperatures of the shape memory alloy used. In this project, A_s , which is the start of Austenite formation on heating, and A_f , which is the finish of the transformation to Austenite, are determined for one type of 55/45 Nitinol compression spring by in situ observation of its shape recovery process.

1.1.2 Critical Review of Previous Work

A substantial number of papers and books have been published on subject of shape memory effect. Given the limited scope of this study, and the abundance of information available on the subject, the critical review of literature was primarily focused on those publications describing the characterization technique of shape memory effect.

Differential Scanning Calorimetry (DSC) is a very useful tool to characterize various phase transformations, and has been widely used to analyze the thermoelastic martensitic transformation in shape-memory alloys by several groups including Francisco M. Braz Fernandes [7], Yongqing Fu [8], T. Lehnert [9] and E.P. George [10]. The DSC method yields a plot such as Figure 2 by measuring the amount of heat given off or absorbed by a tiny sample of the alloy as it is cooled or heated through its phase transformations.

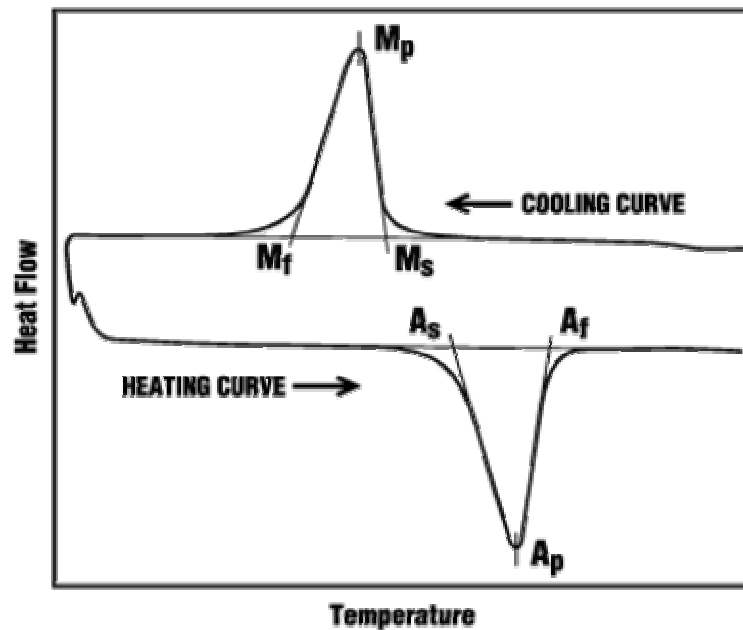


Figure 2: A typical DSC curve for NiTi Shape Memory Alloy [1]

As Darel Hodgson points out, one important drawback to the DSC method is that tests on partially cold worked materials, such as those used to optimize superelasticity, can yield poor, inconclusive results. This same drawback also may apply to samples, which have undergone a heat treatment in the range of 400 to 600 °C following cold working. Thus, fully annealed DSC results are often used as the basis for NiTi raw material selection

since they effectively characterize the baseline properties of the material prior to cold working and heat treatment [1].

On the other hand, because the conventional DSC measures only the sum of all the thermal events, there is always a compromise between sensitivity and resolution in almost all the design schemes of the calorimeters. As a result, some important features may be ignored or the results are easily misinterpreted in the cases involving weak transitions or complex transition. Z. G. Wei suggested that Modulated differential scanning calorimetry (MDSC) technique can provide more valuable information than conventional DSC and can better characterize the first-order and second-order transformations in the alloys. However, the interpretation of the MDSC data remains open and more systematic measurements and theoretical considerations are needed.

Active A_f test, also known as a water bath or alcohol bath test, is another technique used often in the industry [11]. This test is conducted by merely bending a sample of the alloy, such as a wire, while it is below M_s and then monitoring the shape recovery while it is heated. A typical curve is shown in Figure 3. This method, while not very sophisticated, will yield surprisingly accurate, repeatable results if performed carefully, and it requires very little experimental apparatus.

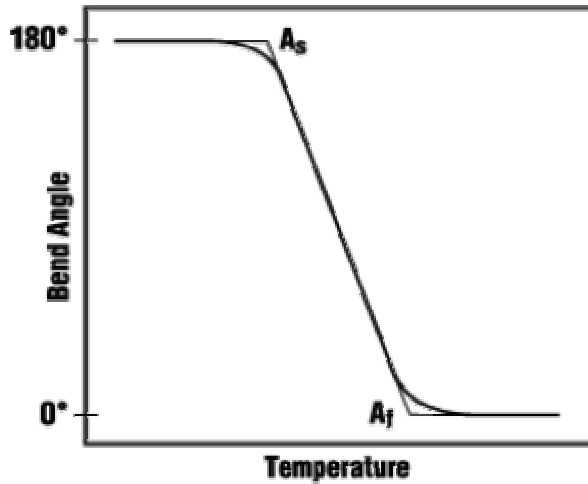


Figure 3: A typical active A_f test curve [1]

Jose Maria Gallardo Fuentes [12], Prahlad, H [13] and F. Trochu [14], performed strain recovery tests to characterize shape memory effect. This method is used to determine and name transformation temperatures by thermally cycling a specimen under loading, producing a T- ϵ curve, as shown in Figure 4. The temperature points noted are ones frequently used to describe the behavior of a particular alloy. M_s is where the Martensite starts to form on cooling and M_f is where Martensite finishes; A_s marks the start of Austenite formation on heating while A_f identifies the finish of the transformation to Austenite and completion of shape recovery.

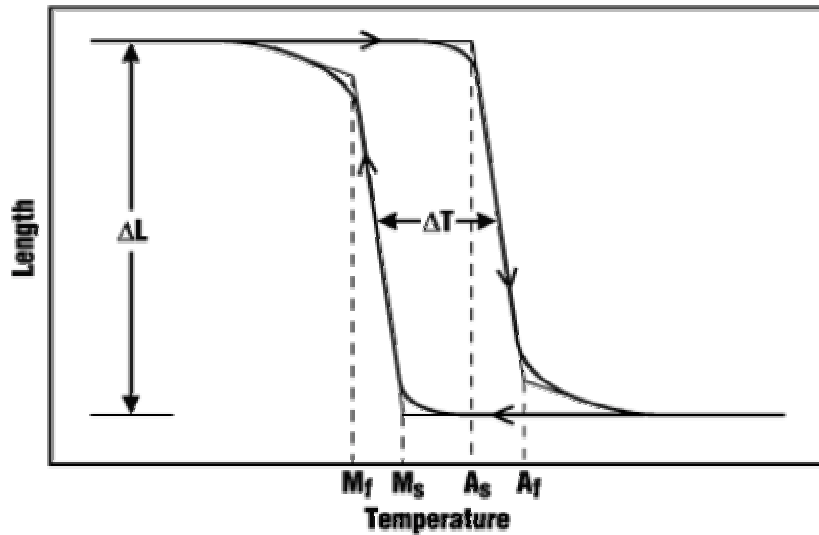


Figure 4: A typical strain recovery test curve

Most of the transformation occurs over a relatively narrow temperature range, although the beginning and end of the transformation during heating or cooling actually extends over a much larger temperature range. The transformation also exhibits hysteresis in that the transformations on heating and on cooling do not overlap. This is the technique selected for the present study.

1.2 Experimental

1.2.1 Experimental Setup

The experiment setup schema was represented in Figure 5. The actual experiment setup was shown on Figure 6.

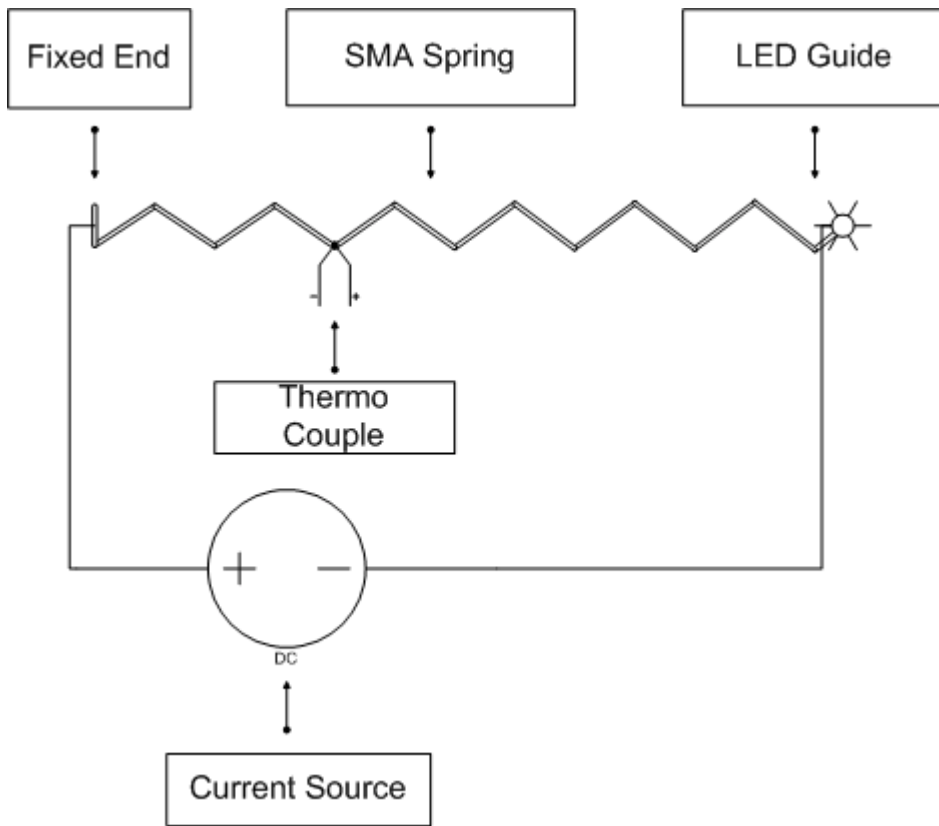
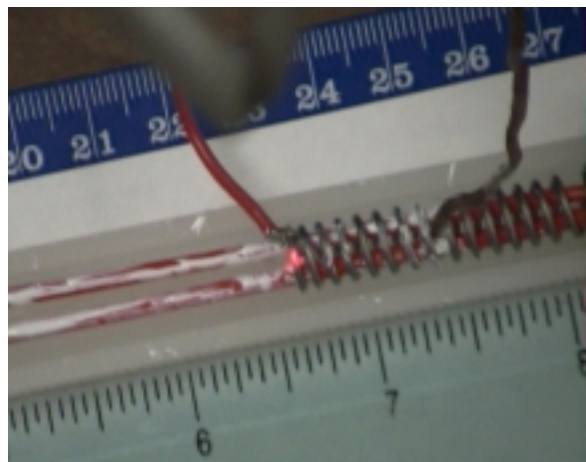


Figure 5: Schema for the experiment setup



(a)



(b)

Figure 6: 6a shows the entire experimental setup for measuring the change in length for the $\text{Ni}_{55}\text{Ti}_{45}$ compression spring. 6b shows the laser point on the edge of the spring.

The specimen was heated by an electrical current of given intensity (Joule effect) by using a DC power supply, Protek Model P5050S. Two red coffee straws were placed inside the specimen then placed onto a plastic guide stage where two metallic paper clips were positioned at the ends as center guide for the straw. The length change of the specimen was recorded by a regular ruler with accuracy to 0.1cm. The spring was fixed at one end and a laser pointer was used to point at the other end. As the spring contracted, the laser pointer was adjusted so that it always point at the end of the spring. This was designed to help detect the spring length change. The temperature of the specimen was measured by a thermocouple, 80 TK module attached to a Fluke 75 multimeter, fixed directly on the sample. A thermal joint compound, Thermoalcote, was used to ensure proper heat transfer between the tip of the thermal couple and the specimen.

1.2.2 Experimental Procedure

One 55/45 Nitinol compression spring was elongated to different length and performed tests on due to limitation of access to shape memory springs. The specimen was obtained from Johnson Matthey Inc. The current applied to the specimen was increased at a step of 0.05A until the spring contraction was detected. The current step up rate changed to 0.01A thereafter. On changing of current each time, a waiting period of minimum 3 minutes were applied for the temperature to stabilize. After 3 minutes of stabilization period, the temperature was recorded once it stayed constant for more than 30 seconds allowing a tolerance of +/- 0.1 °C. The length of the compression spring was recorded every time along with the temperature. The specimen came with an original length of

3.7cm. It was then elongated to 10.1cm and 13cm respectively to perform the experiment. Four tests were performed at each elongated length.

1.3 Results

The plot for the 10.1 cm elongated spring shows highly concentrated data points in the temperature region from 35 °C to 50 °C, as can be seen in Figure 6. These concentrations correlate to the 0.05 A intervals that heated the spring to a steady state temperature. However, the temperature region from 50 °C to 70 °C did not obtain a steady state temperature. The length at 10.1 cm stayed constant up until to 37 °C, then it began to change indicating the onset of phase transformation from martensite to austenite. The austenite start and finish temperatures were determined by drawing horizontal tangential lines at lengths 10.1 cm and 3.7 cm, the original length of the spring or the undeformed martensitic phase. Next, a line was drawn tangential to the slope of the data points as seen in Figure 7, and the intersecting lines on the plot will indicate the A_s and A_f temperatures.

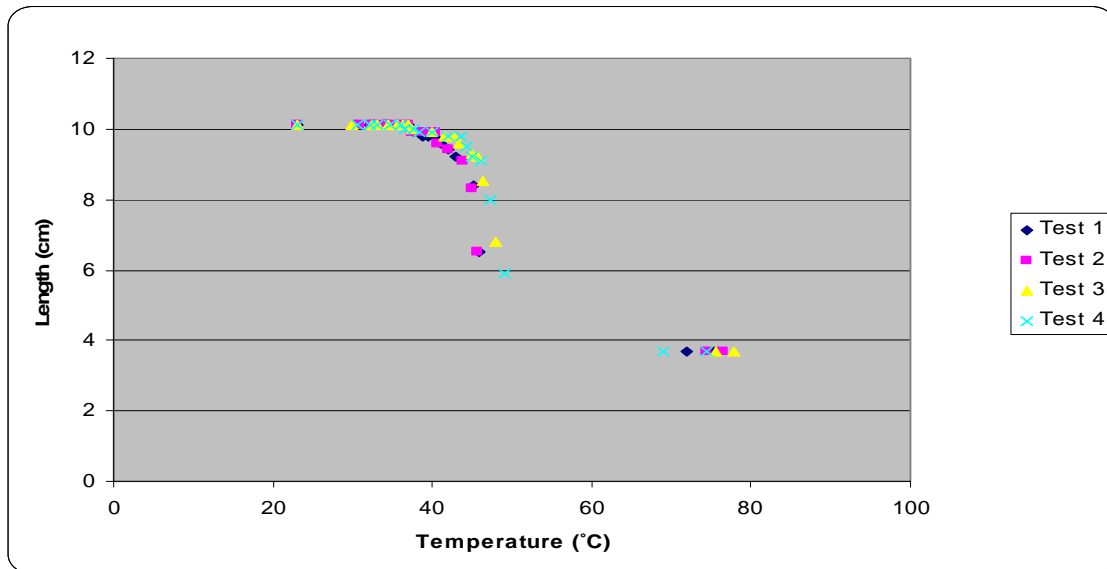


Figure 7: Transformation curve for $Ni_{55}Ti_{45}$ compression spring showing recovery versus temperature. The spring was elongated to 10.1 cm.

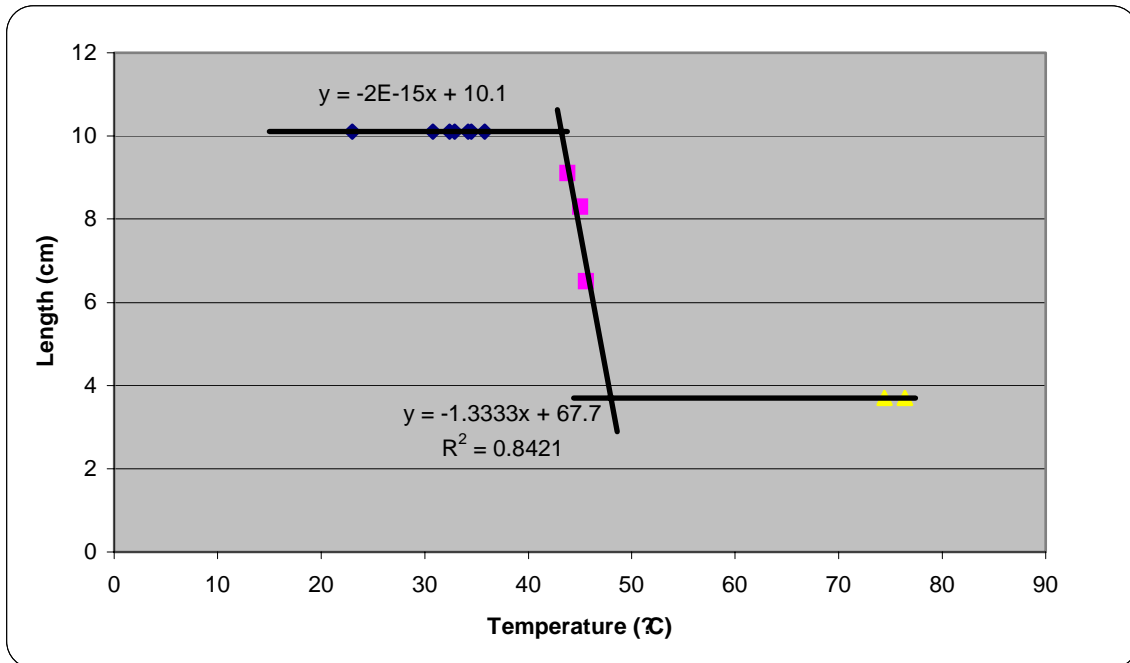


Figure 8. Tangent lines to the data points at 10.1 cm, 3.7 cm and the data point slope. The tangent lines that intersect determines the A_s and A_f temperatures.

For the 13.0 cm elongated spring, the current intervals were changed from 0.05 A to 0.01 A, when the temperature reached approximately 45 °C. As a result a higher concentration of data points can be seen in Figure 8. This plot like Figure 6 shows that the temperature region from about 50 °C to about 74 °C did not reach a steady state temperature, where the spring transformed to its original shape of 3.7 cm. The higher concentration of data points helped to obtain a better determination for the A_s and A_f temperatures. Once the A_s

and A_f temperature were determined for the two elongated springs an overall A_s and A_f average temperature was calculated to be 45.9 °C and 50.4 °C, as can be seen in Table 1.

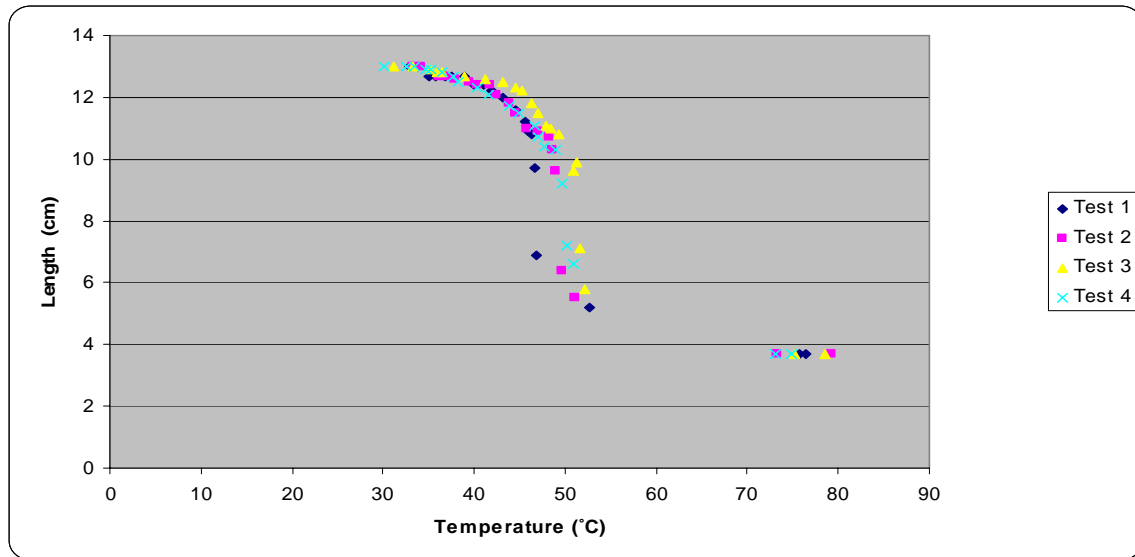


Figure 9: Transformation curve for Ni₅₅Ti₄₅ compression spring showing recovery versus temperature. The spring was elongated to 13 cm.

Table 1. Numerical Calculations for Austenitic Start and Finish Transformation Temperatures.

Compression Spring	A_s	A_f
Ni ₅₅ Ti ₄₅	45.9°C	50.4°C

1.4 Discussion

1.4.1 Statistical Analysis

The A_s temperature range was from 42.1°C to 50 °C or 7.9 °C, which is about 17% of the average. The standard error was the standard deviation divided by the square root of the number of specimen $(2.6 \text{ °C} / 1.4) = 1.8 \text{ °C}$. The 95% confidence range of values would be the Mean $\pm 2*SE$, or A_s : 45.9 ± 3.6 °C. The range for the A_f temperature was from 47.2

°C to 52.7 °C or 5.5 °C, which is about 11% of the value. The standard error was $(1.9 \text{ °C} / 1.4) = 1.3 \text{ C}$ and the 95% confidence range is $50.4 \pm 2.6 \text{ °C}$

1.4.2 Source of Errors

A possible source of error in this experiment could have been from temperature drops. Whenever there was movement in the room the thermocouple would show a drop in temperature, this was especially true when the room was open to the hallway. Another source of error was obtaining measurements in the change of length with a ruler. The best measurement taken was at 1/10 of a centimeter. To try and minimize the measurement errors a laser was used to record changes in spring length. Furthermore, measurements were susceptible to errors if the table was slightly bumped because the stage setup was unstable. The thermo paste for the thermocouple was another possible source of error. The paste would sometimes adhere to the plastic guide, which possibly created a resistance force against the spring, therefore affecting the measurements. In one incident, while the spring was contracting the bonding of the thermocouple to the spring momentarily broke contact, which caused an error in the temperature measurements.

The experimental tests for the two different elongated springs were not consistent and contributed to the poor statistical analysis for the 10.1 cm sample. For the 10.1 cm test, applied current intervals were only at 0.05 A, instead of switching to 0.01 A current intervals when the temperature reached approximately 45 °C, which occurred for the 13.0 cm test as can be seen in Table 2 and Table 3 of the Appendix.

Since A_s and A_f varies substantially with slight change in the composition of the alloy material, no published values were found regarding the specific transformation temperature for this particular Ni₅₅Ti₄₅ compression spring.

1.5 Conclusion

For the Ni₅₅Ti₄₅ compression spring tested, the calculated values for A_s and A_f were 45.9°C and 50.4°C. The work presented in this article shows how A_s and A_f of shape memory alloy can be measured using strain recovery test. Several ideas could be tested to improve this methodology, from experimental point of view:

1. The experiment should be repeated with larger sample size to increase statistical reliability.
2. Various elongated lengths should be tested to verify the validity of the phase transformation temperature.
3. Use Other test methods such as DSC or Active A_f method to confirm results
4. Run the experiment in cooling mode to complete the hysteresis curve

1.6 Acknowledgements

Gordon Arnold: Sierra Monitor Corporation: Special thanks to Gordon Arnold for providing material for the shape memory effect demo, and the use of the laboratory equipment.

Edward Hague: Sierra Monitor Corporation: Special thanks to Edward Hague for providing ideas for test methods

Darel E. Hodgson, Ph.D.: Special thanks supplying the Nitonal springs

Silvie Troung: Johnson Matthey: Special thanks to Silvie for giving us guidance and useful references for project

1.7 References

1. Darel E. Hodgson and Jeffery W. Brown, Johnson Matthey, “Using Nitinol Alloys” (2000)
2. M. Fremond, Shape Memory Alloys, (Springer-Verlag Wien, New York, 1996), pp 71-75
3. Zhao, Chenxu, “*Shape Memory STAINLESS STEELS*”, *Advanced Materials & Processes* **v159, n2**, 33 (2001)
4. S. Miyazaki and L. Otsuka, *Shape Memory Alloys*, ed H. Funakubo, Gordon and Breach Science Publishers, 1987, pp. 116.
5. Zhao, Chenxu, “*Shape Memory STAINLESS STEELS*”, *Advanced Materials & Processes* **v159, n2**, 34(2001)
6. Falcioni, John G., “*Shape memory alloys*”, *Mechanical Engineering-CIME* **v114, n4**, 114(1992)

7. Braz Fernandes, F.M.; Martins, R.; Teresa Nogueira, M.; Silva, R.J.C.; Nunes, P.; Costa, D.; Ferreira, I.; Martins, R. “*Structural characterisation of NiTi thin film shape memory alloys*”. Sensors and Actuators A (Physical), **vol.A99**, (no.1-2), (E-MRS Proceedings of Symposium J: Materials in Microtechnologies and Microsystems, Strasbourg, France, 5-8 June 2001.) April 2002. p.55-8.
8. Yongqing Fu; Weimin Huang; Hejun Du; Xu Huang; Junping Tan; Xiangyang Gao, “*Characterization of TiNi shape-memory alloy thin films for MEMS applications*”. Surface & Coatings Technology, vol.**145**, (no.1-3), pp.107-12(2001)
9. E. P. George, C. T. Liu, J. A. Horton, C. J. Sparks, M. Kao, H. Kunsmann, and T. King, “*Characterization, Processing and Alloy Design of NiAl-Based Shape Memory Alloys*”, Materials Characterization **21**, 139-160(1994)
10. T. Lehnert, H. Grimmer, P. Boni, M. Horisberger and R. Gotthardt, “*Characterization of Shape-Memory Alloy Thin Films Made Up From Sputter-Deposited Ni/Ti Multilayers*”, Acta Materialia, No. **48**. pp. 4065-4071(2000)
11. .Ochin, P.; Dezellus, A.; Plaindoux, P.; Portier, R.; Pons, J.; Cesari, E.; Kozlov, A., “*Preparation and characterization of Cu-based shape-memory thin wires obtained by in rotating water melt-spinning*”. Materials Science Forum, vol.**394-395**, (Shape Memory Materials and Its Applications. International Conference on Shape Memory and Superelastic Technologies and Shape Memory and Superelastic Technologies and Shape Memory Materials (SMST-SMM 2001), Kunming, China, 2-6 Sept. 2001.) Trans Tech Publications, 2002. p.503-6.

12. Jose Maria Gallardo Fuentes, Paul Gumpel, Joachim Stittmatter, “*Phase change behavior of Nitinol Shape Memory Alloys*”, *Advanced Engineering Materials*, No. **7**, pp.441- 451 (2002)
13. Prahlad, H.; Chopra, I., “*Experimental characterization of Ni-Ti shape memory alloy wires under complex loading conditions.*” , Proceedings of the SPIE - The International Society for Optical Engineering, vol.3668, pt.1-2, (Smart Structures and Materials 1999: Smart Structures and Integrated Systems, Newport Beach, CA, USA, 1-4 March 1999.) SPIE-Int. Soc. Opt. Eng, 1999. p.604-16.
14. F. Trochu, N. Sacepe, O. Volkov, S. Turenne, “*Characterization of NiTi shape memory alloys using dual Kriging interpolation*”, *Material Science and Engineering* **A273-275**, pp. 395-399 (1999)

Appendix

Table 2. Data Measurements for the 10.1 cm Elongated Ni₅₅Ti₄₅ Compression Spring.

10.1 cm	current	voltage	Temperature +/- .1C	dL (cm)	length (cm)	10.1 cm	curren t	voltage	Temperature +/- .1C	dL (cm)	length (cm)
Test 1	0	0	23	0	10.1	Test 3	0	0	23	0	10.1
	1.05	0.7	30.8	0	10.1		1.05	0.7	30	0	10.1
	1.1	0.7	32.4	0	10.1		1.1	0.7	32.4	0	10.1
	1.15	0.7	32.9	0	10.1		1.15	0.7	33	0	10.1
	1.2	0.8	34.2	0	10.1		1.2	0.8	34.5	0	10.1
	1.25	0.8	34.5	0	10.1		1.25	0.8	35.7	0	10.1
	1.3	0.8	35.8	0	10.1		1.3	0.8	36.3	0	10.1
	1.35	0.9	37.1	0	10.1		1.35	0.9	36.9	0	10.1
	1.4	0.9	37.5	0.2	9.9		1.4	0.9	37.5	0.1	10
	1.45	0.9	38.3	0.2	9.9		1.45	0.9	40	0.2	9.9
	1.5	0.9	39.3	0.2	9.9		1.5	0.9	41.5	0.3	9.8
	1.55	1	40.3	0.2	9.9		1.55	1	42.6	0.3	9.8
	1.6	1	40.7	0.5	9.6		1.6	1	43.3	0.5	9.6
	1.65	1	42.1	0.7	9.4		1.65	1	44.9	0.8	9.3
	1.7	1.1	43.8	1	9.1		1.7	1.1	45.6	0.9	9.2
	1.75	1.1	45	1.8	8.3		1.75	1.1	46.3	1.6	8.5
	1.8	1.1	45.6	3.6	6.5		1.8	1.1	48	3.3	6.8
	1.85	1.1	74.4	6.4	3.7		1.85	1.1	75.6	6.4	3.7
	1.9	1.1	76.4	6.4	3.7		1.9	1.1	77.9	6.4	3.7
Test 2	0	0	23	0	10.1	Test 4	0	0	23	0	10.1
	1.05	0.7	30.4	0	10.1		1.05	0.7	30.5	0	10.1
	1.1	0.7	32.1	0	10.1		1.1	0.7	32.2	0	10.1
	1.15	0.7	32.7	0	10.1		1.15	0.7	33.1	0	10.1
	1.2	0.8	34	0	10.1		1.2	0.8	34.7	0	10.1
	1.25	0.8	34.5	0	10.1		1.25	0.8	36	0	10.1
	1.3	0.8	35.7	0	10.1		1.3	0.8	36.6	0.1	10
	1.35	0.9	37.1	0	10.1		1.35	0.9	37.7	0.1	10
	1.4	0.9	37.7	0.2	9.9		1.4	0.9	38.4	0.2	9.9
	1.45	0.9	38.8	0.3	9.8		1.45	0.9	40	0.2	9.9
	1.5	0.9	39.6	0.3	9.8		1.5	0.9	41.9	0.3	9.8
	1.55	1	40.6	0.4	9.7		1.55	1	43.5	0.3	9.8
	1.6	1	41	0.5	9.6		1.6	1	44.2	0.6	9.5
	1.65	1	41.9	0.7	9.4		1.65	1	44.9	0.9	9.2
	1.7	1.1	43	0.9	9.2		1.7	1.1	46.1	1	9.1
	1.75	1.1	45.1	1.7	8.4		1.75	1.1	47.3	2.1	8
	1.8	1.1	45.8	3.6	6.5		1.8	1.1	49.1	4.2	5.9
	1.85	1.1	72	6.4	3.7		1.85	1.1	69	6.4	3.7
	1.9	1.1	75.4	6.4	3.7		1.9	1.1	74.5	6.4	3.7

Table 3. Data Measurements for the 13.0 cm Elongated Ni₅₅Ti₄₅ Compression Spring.

13.0 cm	current	voltage	Temperature +/- .1C	dL (cm)	length (cm)	13.0 cm	current	voltage	Temperature +/- .1C	dL (cm)	length (cm)
Test 1	1.15	0.8	32.9	0	13	Test 3	1.15	0.8	31.1	0	13
	1.2	0.8	33.8	0	13		1.2	0.8	33.2	0	13
	1.25	0.8	35.1	0.3	12.7		1.25	0.8	35.3	0.1	12.9
	1.3	0.8	35.8	0.3	12.7		1.3	0.8	36	0.2	12.8
	1.35	0.9	36.8	0.3	12.7		1.35	0.9	36.5	0.2	12.8
	1.4	0.9	37.6	0.3	12.7		1.4	0.9	39	0.3	12.7
	1.45	0.9	38.9	0.3	12.7		1.45	0.9	41.2	0.4	12.6
	1.5	0.9	39.9	0.6	12.4		1.5	0.9	43.1	0.5	12.5
	1.55	1	41	0.6	12.4		1.55	1	44.6	0.7	12.3
	1.6	1	42	0.8	12.2		1.6	1	45.3	0.8	12.2
	1.65	1	43.2	1	12		1.65	1	46.4	1.2	11.8
	1.7	1	44.6	1.4	11.6		1.7	1	47.1	1.5	11.5
	1.75	1	45.6	1.8	11.2		1.75	1	47.9	1.9	11.1
	1.76	1	45.8	1.9	11.1		1.76	1	48.5	2	11
	1.77	1	46	2.1	10.9		1.77	1	49.4	2.2	10.8
	1.78	1	46.4	2.2	10.8		1.78	1	50.9	3.4	9.6
	1.79	1	46.6	3.3	9.7		1.79	1	51.2	3.1	9.9
	1.8	1.1	46.8	6.1	6.9		1.8	1.1	51.6	5.9	7.1
	1.81	1.1	52.6	7.8	5.2		1.81	1.1	52.2	7.2	5.8
	1.82	1	75.7	9.3	3.7		1.82	1	75.2	9.3	3.7
	1.83	1	76.4	9.3	3.7		1.83	1	78.6	9.3	3.7
Test 2	1.15	0.8	33.2	0	13	Test 4	1.15	0.8	30.2	0	13
	1.2	0.8	34.1	0	13		1.2	0.8	32.6	0	13
	1.25	0.8	36.1	0.3	12.7		1.25	0.8	33.4	0	13
	1.3	0.8	36.4	0.3	12.7		1.3	0.8	34.7	0.1	12.9
	1.35	0.9	36.8	0.3	12.7		1.35	0.9	35.2	0.1	12.9
	1.4	0.9	37.9	0.4	12.6		1.4	0.9	36.4	0.2	12.8
	1.45	0.9	39.5	0.5	12.5		1.45	0.9	37.7	0.3	12.7
	1.5	0.9	40.3	0.6	12.4		1.5	0.9	38.2	0.5	12.5
	1.55	1	41.7	0.6	12.4		1.55	1	40.3	0.7	12.3
	1.6	1	42.4	0.9	12.1		1.6	1	41.6	0.9	12.1
	1.65	1	43.9	1.2	11.8		1.65	1	43.9	1.3	11.7
	1.7	1	44.5	1.5	11.5		1.7	1	44.9	1.5	11.5
	1.75	1	45.8	2	11		1.75	1	46.6	1.9	11.1
	1.76	1	47	2.1	10.9		1.76	1	47.1	2.3	10.7
	1.77	1	48.2	2.3	10.7		1.77	1	47.8	2.6	10.4
	1.78	1	48.6	2.7	10.3		1.78	1	48.9	2.7	10.3
	1.79	1	49	3.4	9.6		1.79	1	49.7	3.8	9.2
	1.8	1.1	49.7	6.6	6.4		1.8	1.1	50.2	5.8	7.2
	1.81	1.1	51	7.5	5.5		1.81	1.1	50.9	6.4	6.6
	1.82	1	73.3	9.3	3.7		1.82	1	73.1	9.3	3.7
	1.83	1	79.2	9.3	3.7		1.83	1	74.9	9.3	3.7